TERMINAL CONTROL OF A 2-LINK ROBOT MANIPULATOR

Josep Mª de Castro, Paula Domínguez Pla, and Nil Palau
PEF2 Project
Polytechnic University of Catalonia
C. Jordi Girona, 31
Barcelona, 08034
Spain

(Dated: June 4, 2021)

ABSTRACT

This paper describes a comparative evaluation of different controllers for a position regulation 2-link robot manipulator. The equation of motion for two link robot is a nonlinear differential equation. The controllers, namely two proportional plus derivative with a nonlinear compensation and a terminal control, are designed from the dynamic description of the two link robot and then the controlled system is simulated by means of Matlab/Simulink software which allows animated simulations using 3D World Editor (Matlab).

I. INTRODUCTION

It is well known that robot manipulators are highly nonlinear, dynamically coupled and time-varying systems which are extensively used in industries. Furthermore, robotic manipulators are generally subjected to uncertainties. Because of these uncertainties and nonlinear behavior, it's a challenging task to control the motion of robot manipulator to an accurate position.
This work is based in several articles which deal with the terminal control of nonlinear systems ([1],[3],[4]). In it, the robot dynamics and the controllers design will be presented for a later simulation, from which the results and conclusions will be obtained. Finally, to better understand the results, a 3D animation of the robot will be created.

II. ROBOT DYNAMICS

The 2-link robot arm studied is shown in Fig 1:

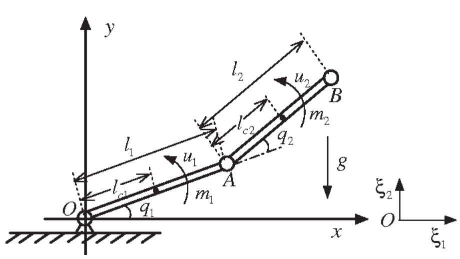

FIG. 1: 2-link robot arm. (Figure from ([5]))

The method for deriving the dynamic equations of mechanical systems is via Euler-Lagrange equation:

$$\frac{d}{dt}\frac{\partial L}{\partial \dot{\mathbf{q}}} - \frac{\partial L}{\partial \mathbf{q}} = \tau,$$

where $\mathbf{q} = (q_1, q_2)$, L is the Lagrangian of the system and τ are the generalized forces that act upon the system.
By solving the Euler-Lagrange equation, as in [1] and [2], the robot dynamics system of equations is :

$$H(\mathbf{q})\ddot{\mathbf{q}} + C(\mathbf{q}, \dot{\mathbf{q}})\dot{\mathbf{q}} + \mathbf{g}(\mathbf{q}) = \tau. \tag{1}$$

From Reyes et. all 1997 [1], the entries of the robot dynamics are:

$$H(\mathbf{q}) = \begin{pmatrix} \theta_1 + 2\theta_2\cos(q_2) & \theta_3 + \theta_2\cos(q_2) \\ \theta_3 + \theta_2\cos(q_2) & \theta_3 \end{pmatrix}, \tag{2}$$

$$C(\dot{\mathbf{q}}, \mathbf{q}) = \begin{pmatrix} -2\theta_2\cos(q_2)\dot{q}_2 & -\theta_2\cos(q_2)\dot{q}_2 \\ \theta_2\cos(q_2)\dot{q}_1 & 0 \end{pmatrix}, \tag{3}$$

$$\mathbf{g}(\mathbf{q}) = \begin{pmatrix} \theta_4\sin(q_1) + \theta_5\sin(q_1 + q_2) \\ \theta_5\sin(q_1 + q_2) \end{pmatrix}, \tag{4}$$

with:

$$\begin{cases} \theta_1 = m_1 l_{c1}^2 + m_2 l_1^2 + m_2 l_{c2}^2 + I_1 + I_2 \\ \theta_2 = l_1 m_2 l_{c2} \\ \theta_3 = m_2 l_{c2}^2 + I_2 \\ \theta_4 = g(l_{c1}m_1 + m_2 l_1) \\ \theta_5 = g m_2 l_{c2} \end{cases}$$

As a consequence, the robot dynamics can be expressed as a order two system, defining x_1 as a vector composed of both angles and x_2 the vector of the angular velocities:

$$\begin{cases} \dot{x}_1 = x_2 \\ \dot{x}_2 = H(x_1)^{-1}\Big(\tau - C(x_1, x_2)x_2 - g(x_1)\Big). \end{cases} \tag{5}$$

Hence, the equilibrium points of the system are:

$$x_1^* = x_1^d \qquad \& \qquad x_2^* = 0.$$

Therefore, redefining the system in terms of the errors, we obtain:

$$\begin{cases} \dot{e}_1 = e_2 \\ \dot{e}_2 = H(e_1 + x_1^d)^{-1}\Big(\tau - C(e_1 + x_1^d, e_2)e_2 - g(e_1 + x_1^d)\Big), \end{cases} \tag{6}$$

where $e_1 = x_1 - x_1^d$ and $e_2 = x_2$.

III. CONTROLLER DESIGN

This section provides the controller formulation along with its integration with the system dynamics. Three different controllers are considered, two different controllers with a proportional and derivative term (PD) and non-linear compensation terms and a terminal sliding mode controller.

A. PD controller

The PD controller is given by:

$$\tau = H(x_1)(-K_P e_1 - K_D e_2) + C(x_1, x_2)x_2 + g(x_1), \quad (7)$$

where K_P and K_D represent the proportional and derivative gain diagonal matrices.
For simplification purposes the parameters are set as $K_{P1} = K_{P2} = K_P$ and $K_{D1} = K_{D2} = K_D$. Therefore, the closed-loop system (6) becomes:

$$\begin{cases} \dot{e}_1 = e_2 \\ \dot{e}_2 = -K_P e_1 - K_D e_2. \end{cases} \quad (8)$$

The closed-loop stability is checked by means of the following Lyapunov function candidate:

$$V = \frac{1}{2}\Big(e_2^T e_2 + e_1^T K_P e_1\Big),$$

which is globally positive definite, in turn:

$$\dot{V} = e_2^T \dot{e}_2 + e_1^T K_P \dot{e}_1 = e_2^T(-K_P e_1 - K_D e_2) + e_1^T K_P e_2$$

$$\dot{V} = -e_2^T K_D e_2 \ < 0 \ \ \forall \mathbf{x} \setminus \{x_2 = 0\}.$$

Applying LaSalle's theorem, $R = \{\mathbf{e} \in \mathbb{R}^2;\ \dot{V} = 0\} = \{(e_1, 0)\}$. The largest invarient set within R is given by $M = \{\mathbf{e} \in \mathbb{R}^2;\ e_2 = \dot{e}_2 = 0\}$, and

$$\dot{e_2}\Big|_{e_2=0} = -K_P e_1 - K_D e_2\Big|_{e_2=0} = -K_P e_1 = 0$$

$$\Rightarrow e_1 = 0 \Rightarrow \dot{e}_1 = 0.$$

Therefore, the largest invariant set is $M = \{0\}$. By the Corollary of LaSalle's invariance principle this is an asymptotically stable equilibrium of the system.
It is also demonstrated to be a globally asymptotically stable equilibrium:

$$V = \frac{1}{2}\Big(e_2^T e_2 + e_1^T K_P e_1\Big) \leq \frac{1}{2}\lambda ||e||^2 \xrightarrow{||e||^2 \to \infty} \infty.$$

The system of ordinary differential equations is solved by using ode4 solver in Matlab/Simulink environment. The block diagram for this control is shown on figure (2).
The first three blocks, starting from the left side of the block diagram, describe the control block while the last one implements the non-linear differential equation of the robot's dynamics.

B. PD controller v.2

This second PD controller does not include the inertia matrix on its description, in such a way that stability is not as easily demonstrated.
The controller studied is given by:

$$\tau = -K_P e_1 - K_D e_2 + C(x_1, x_2)x_2 + g(x_1). \quad (9)$$

Therefore, the closed-loop system in terms of the error becomes:

$$\begin{cases} \dot{e}_1 = e_2 \\ \dot{e}_2 = -H(e_1 + x_1^d)^{-1}\Big(K_P e_1 + K_D e_2\Big). \end{cases} \quad (10)$$

Hence, the Lyapunov function candidate:

$$V = \frac{1}{2}\Big(e_2^T H(x_1) e_2 + e_1^T K_P e_1\Big),$$

which is globally positive definite, its derivative cannot be proven negative definite. Therefore, stability will be demonstrated locally by linearizing around the equilibrium.
Defining the components of the error vectors:

$$e_1 = [\epsilon_1,\ \epsilon_2]^T \qquad \& \qquad e_2 = [\dot{\epsilon}_1,\ \dot{\epsilon}_2]^T,$$

the linearized system of order 4 around $x_1^* = x_1^d$ and $x_2^* = 0$, that is to say, around $e_1 = 0$ and $e_2 = 0$, is:

$$\begin{bmatrix} \dot{\epsilon}_1 \\ \dot{\epsilon}_2 \\ \ddot{\epsilon}_1 \\ \ddot{\epsilon}_2 \end{bmatrix} = \begin{bmatrix} 0 & 0 & 1 & 0 \\ 0 & 0 & 0 & 1 \\ -\frac{K_P\theta_3}{D} & \frac{K_P\alpha}{D} & -\frac{K_D\theta_3}{D} & \frac{K_D\alpha}{D} \\ \frac{K_P\alpha}{D} & -\frac{K_P\beta}{D} & \frac{K_D\alpha}{D} & -\frac{K_D\beta}{D} \end{bmatrix} \begin{bmatrix} \epsilon_1 \\ \epsilon_2 \\ \dot{\epsilon}_1 \\ \dot{\epsilon}_2 \end{bmatrix}, \quad (11)$$

where $D = \frac{1}{\theta_3\theta_1 - \theta_3^2 - \theta_2^2\cos^2 q_2^d}$, $\alpha = \theta_3 + \theta_2 \cos q_2^d$ and $\beta = \theta_1 + 2\theta_2 \cos q_2^d$.
Finding the characteristic polynomial and applying Routh's criterion, the stability of the system for any desired position remains within the shaded region of combinations of K_P and K_D of figure (3).
From figure (3), we are able to guarantee local asymptotic stability near the equilibrium for certain values of the proportional and derivative gain parameters.
The block diagram for this controller is shown on figure (2), the difference from both controllers is the appearance of the inertia matrix in block *Calcul_tau*, and is thereafter solved by using ode4 in Matlab/Simulink environment.

C. Terminal controller

The last controller is a type of terminal controller which makes use of a sliding surface. The design of the control switch surface in Terminal sliding mode (TSMC) can be performed with the objective of adding properties to the resulting dynamics beyond the characteristic of convergence to the steady state in finite time ([4],[3]). Therefore, our main aim is to find an expression for τ such that the angles reach the desired position assymptotically and that the error, $e = x - x^d$, approaches zero at an exponential rate.

$$e \to 0 \ \text{ as } \ t \to \infty$$

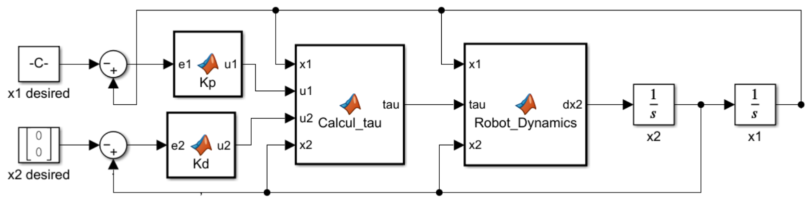

FIG. 2: PD control Block Diagram

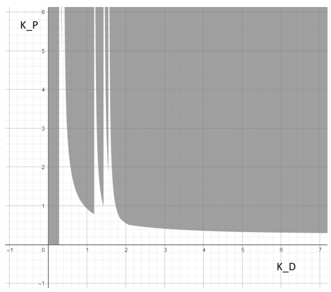

FIG. 3: Stability region for different K_P and K_D values

Defining the sliding surface as:

$$s_t = \lambda e_1^\gamma + \dot{e_1} = \lambda e_1^\gamma + e_2,$$

the former parameters must satisfy the following conditions: $\lambda > 0$ and $0 < \gamma = \frac{n}{d} < 1$, where n and d are odd positive integers.
The sliding dynamics obtained on the terminal structure sliding surface is given by the imposition: $s_t = 0$.

$$s_t = 0 \;\Rightarrow\; \dot{e}_1 = -\lambda e_1^\gamma$$

$$e_1(t) = \sqrt[1-\gamma]{-\lambda(1-\gamma)t + |e_1(0)|^{1-\gamma}}$$

The system reaches $e_1 = 0$ at a finite time, t_s:

$$t_s = \frac{|e_1(0)|^{1-\gamma}}{\lambda(1-\gamma)}.$$

Computing the first derivative of the sliding surface, in such a way that, the control term τ appears and is generated to cancel out the terms of $\dot{s}_t$:

$$\dot{s}_t = \lambda\gamma e_1^{\gamma-1}\dot{e}_1 + \ddot{e}_1.$$

Replacing the expressions of $\dot{e}_1$ and $\dot{e}_2$ found in (10) and going back to the initial variables (x_1,x_2), the previous equation reads:

$$\dot{s}_t = \lambda\gamma(x_1 - x_1^d)^{\gamma-1}x_2 + H(x_1)^{-1}\Big(\tau - C(x_1, x_2)x_2 - g(x_1)\Big).$$

Therefore, selecting τ such as:

$$\tau = C(x_1, x_2)x_2 + g(x_1) - H(x_1)\lambda\gamma(x_1 - x_1^d)^{\gamma-1}x_2.$$

Choosing the following positive definite Lyapunov function candidate:

$$V = \frac{s_t^2}{2} \quad \rightarrow \quad V = s_t\dot{s}_t = 0.$$

Hence, to guarantee stability an extra term is incorporated to the control definition:

$$\tau = C(x_1, x_2)x_2 + g(x_1) - H(x_1)(\lambda\gamma(x_1 - x_1^d)^{\gamma-1}x_2 + \eta sign(s)),$$

where η is able to control the instant at which the desired position is reached $t_{reach} \leq \frac{|s_t(0)|}{\eta}$, and therefore, is chosen in such a way that the desired position is reached in a certain time.
The system of ordinary differential equations is solved by using ode4 solver in Matlab/Simulink environment. The block diagram for this control is shown on figure (4).

IV. RESULTS AND DISCUSSION

Using Matlab/Simulink environment we have evaluated the performance of our results in simulations. The total simulation time is $T = 20$ s with a sampling time of $t_s = 0.001$ s. For simulation, the system parameters selected are those of Table 1 (Reyes et. all, 1997, p.567) [1].

Parameter	Notation	Value	Unit
Length link 1	l_1	0.45	m
Mass link 1	m_1	23.902	Kg
Mass link 2	m_2	10.880	Kg
Length link 1	l_{c_1}	0.225	m
Length link 2	l_{c_2}	0.1	m
Inertia link 1	I_1	1.266	$Kg\ m^2$
Inertia link 2	I_2	0.493	$Kg\ m^2$
Gravity acceleration	g	9.81	m/s^2

TABLE I: Parameter values. (Table from [1])

All controls will be simulated starting from a given initial position, with null initial speed, i.e.,

$$q_{1,0} = \pi \qquad q_{2,0} = 0.3\pi \qquad \dot{q}_{1,0} = \dot{q}_{2,0} = 0$$

which imply nonzero initial position errors.
And, therefore, will end in a desired position, i.e,

$$q_1^d = \frac{\pi}{3} \qquad q_2^d = \frac{11\pi}{6} \qquad \dot{q}_1^d = \dot{q}_2^d = 0$$

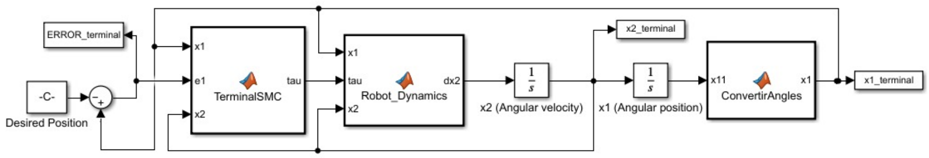

FIG. 4: TSMC Block Diagram

In the following figure we can see, qualitatively, how the different values of the PD control parameters affect the behavior of our system. Following this idea, several similar tests have been carried out to find those values of K_P and K_D which ensure the desired behavior of the robot.

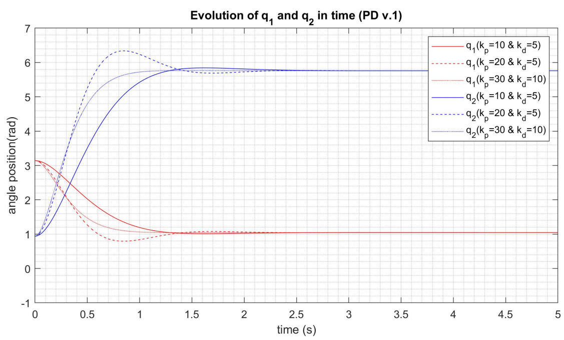

FIG. 5: Comparison of different control parameters in PD control

It can be seen from figure (5) the proportional gain increases the rise time decreases, moreover, if the derivative gain increases the overshoot also decreses and so does the settling time. Therefore, after many attempts the final parameters have been set to:

Control	$\mathbf{K_P}$	$\mathbf{K_D}$	η
PD v.1	30	10	-
PD v.2	30	10	-
SMC	-	-	25

TABLE II: Control Parameters

The response using the PD controller is depicted in figure (6), it is clear that the PD controller v.1 takes at least 2.5 seconds to bring the arm at the desired position with maximum control. The second PD controller has a slower response but is as well capable of taking the robot arm to the desired position. The SMC, on other hand, is capable of moving the arm to the desired position in less than 2 seconds (see in figure (6)).
Thereafter, to interactively visualize the movement of the robotic arm, we have implemented a 3D animation using

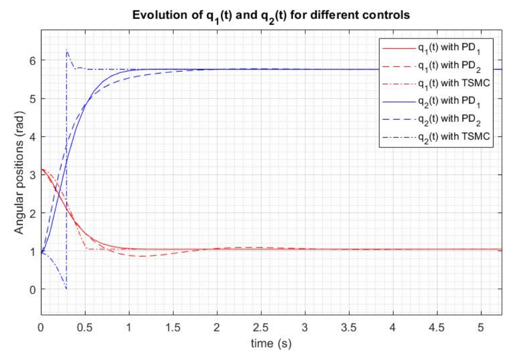

FIG. 6: Temporal response of the three different controls

Simulink/3D World Editor from Matlab's environment. This animation is linked to the Simulink simulation result and therefore perfectly captures the theoretical trajectory of the arm. An image of the 3D animation is shown on figure (7).

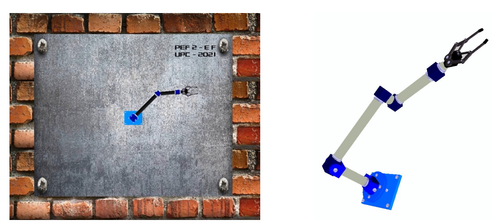

FIG. 7: 3D animation of the robot arm

V. CONCLUSIONS

In this article, a robust control based on the conventional sliding mode controller has been introduced to control the motion of the two-link robotic arm at specific position, and it has been compared with two different PD controls. The obtained results have shown that the SMC outperform the PD controller in terms of fast and robust response though with higher control signal. The high joint speeds in case of SMC, which are a consequence of high control signal in this case, are required for rapid movement of the links. It is expected that adaptive SMC control may lead to a better response.

REFERENCES

[1] Reyes, F. & Kelly, R. (1997). Experimental Evaluation of Identification Schemes on a Direct Drive Robot. *Robotica. 15(5).* 563-571. doi:10.1017/S0263574797000659.

[2] Ortega, R. & Spong, M.W. (1998). Adaptative motion control of rigid robots: A tutorial. *Autom., 25*, 877-888.

[3] Venkataraman, S.T. & Gulati, S. (1992). Control of Nonlinear Systems Using Terminal Sliding Modes. *American Control Conference, 1992*, pp. 891-893, doi: 10.23919/ACC.1992.4792209.

[4] Masclans, N., Repecho, V. & Biel, D. (2019). Control en modo deslizante terminal con limitación de corriente en arranque en un convertidor reductor. *A: Seminario Anual de Automática, Electrónica Industrial e Instrumentación. "XXVI Seminario Anual de Automática, Electrónica Industrial e Instrumentación: libro de resúmenes, Córdoba 3-5 julio 2019".* p. 583-588.

[5] Cui, M., Wu, Z., & Xie, X. (2013). *TRACKING CONTROL FOR A TWO-LINK PLANAR RIGID ROBOT MANIPULATOR.*